

Extinction in Nebular Luminosities & Star Formation Rate of Disk Galaxies: Inclination Correction

Ching-Wa Yip & Alex S. Szalay

cwyip@pha.jhu.edu; szalay@jhu.edu

ABSTRACT

Star formation is one of the most important processes in galaxy formation. The luminosity of $H\alpha$ recombination and $[O II]\lambda 3728$ forbidden emissions remain to be most used in measuring formation rate of massive stars in galaxies. Here we report the inclination dependency of continuum-subtracted and aperture-corrected nebular luminosities, including $H\alpha$, $H\beta$, $H\gamma$, $[O II]$, $[N II]$, of disk-dominated galaxies in the local universe. Their luminosities decrease by a factor of three from face-on to edge-on (axis ratio limit = 0.17) orientations. This dependence is deduced to be caused by extinction due to diffuse dust within the disks with an amplitude of 1.2 mag. The line-luminosity-inclination relation provides a novel way to remove extinction in emission lines and present star formation rate of disk galaxies out to redshift of 1.6.

Subject headings: galaxies: fundamental parameters — techniques: spectroscopic — methods: data analysis

1. Motivation

Star formation is one of the most important phenomena during the formation of a galaxy. To measure the star formation rate (SFR), the luminosities of both $H\alpha$ and $[O II]$ are used because they depend on the ionizing photon luminosity (e.g., Eqn. 2 of Kennicutt 1998). The radiation from massive stars, taken to be a blackbody (Zanstra 1927) and determined to arise from O/B stars, is the ionizing source to the H II region gas, or nebular gas. The SFR have been quantified using large samples of galaxies (e.g., Brinchmann et al. 2004) and across cosmic distances (e.g., Lilly et al. 1996; Connolly et al. 1997; Madau et al. 1998; Hopkins & Beacom 2006). On average, star-forming galaxies are dusty (e.g., Calzetti et al.

(2000); Driver et al. (2007); Shao et al. (2007); Holwerda et al. (2007); Unterborn & Ryden (2008); Bailin & Harris (2008); Maller et al. (2009); Masters et al. (2010); Conroy et al. (2010); Wild et al. (2011) and Yip et al. (2010, hereafter Paper I)). It is therefore critical to get SFR free from extinction.

The extinction correction to the spectral energy distribution of disk galaxies can be decomposed into two terms: the inclination-dependent and -independent (e.g., face-on) corrections (see Driver et al. 2008). While the inclination dependency of optical stellar continuum in disk galaxies is established (Driver et al. 2007; Unterborn & Ryden 2008; Bailin & Harris 2008; Maller et al. 2009; Yip et al. 2010), that of individual nebular emissions is still lacking. The goal of this *Letter* is to determine the inclination correction to individual nebular emissions and therefore SFR of disk galaxies. We quantify the luminosity of the $H\alpha$, $H\beta$, $H\gamma$ recombination lines, and the $[O\ II]$, $[N\ II]$ forbidden lines, as a function of inclination for a sample of local disk-dominated galaxies. The line-luminosity–inclination relation can be used to remove inclination-dependent extinction of disk galaxies.

2. Analysis

Our sample is composed of galaxies from the Sloan Digital Sky Survey (SDSS, York et al. 2000) Data Release 6 (DR6, Adelman-McCarthy et al. 2008) that are morphologically disk dominated and spectroscopically star forming. The selection criteria were described in detail in Paper I. To summarize the key characteristics, the sample is (1) within redshifts from 0.065 to 0.075; (2) within r -band Petrosian absolute magnitudes from -19.5 to -22; (3) volume limited, in avoiding the Malmquist bias and (4) showing a uniform distribution of inclination, in avoiding bias in galaxy properties from one inclination to the next. Following Paper I, the inclination of a galaxy is proxied by its r -band axis ratio, with the consideration that the average ellipticity is small (16%, Ryden 2004).

To quantify the line luminosity as a function of inclination, we first construct high signal-to-noise composite spectrum, at a spectral resolution of 70 km s^{-1} , in bins of inclination (Table 2). We then measure the continuum-subtracted line luminosities in the composites. The methodologies in continuum estimation and line fitting were discussed in Paper I. Finally, we apply an aperture correction to obtain line luminosities that are expected from the whole galaxies. The correction is specifically developed in this work for the purpose of inclination studies with fiber spectroscopy.

The SDSS spectra of the galaxies are downloaded through the Spectrum Services (Dobos et al. 2004). Line luminosities are expressed in $10^{40}\text{ erg s}^{-1}$, and the vacuum wavelength conven-

tion is used throughout the analysis. The flux-to-luminosity conversion made use of the cosmological parameters $\Omega_V = 0.73$, $\Omega_M = 0.27$, and $h = 0.71$.

2.1. Aperture Correction

The SDSS spectroscopic fiber is $1.5''$ in radius ($r_{\text{fiber}} = 1.5''$), which measures 0.5 half-light radius area on our disk galaxies (see Table 1 and §2.1.1). A two-step procedure is developed to obtain line luminosities of the whole galaxies from the observed luminosities through the fiber. First, the fiber luminosity is converted to the central luminosity within a radius, r_{circle} , on the plane of a galaxy (hereafter, the step *Fiber-to-Circle*). Second, this central luminosity is converted to the luminosity of the whole galaxy (the step *Circle-to-Total*).

2.1.1. Step 1: Fiber-to-Circle Correction

When a disk galaxy is inclined, a circular spectroscopic fiber measures an elliptical area *on the plane of the disk*, rather than a circular area. The luminosity through the spectroscopic fiber is contributed not only from all of the isophotes within the radius $r_{\text{circle}} = r_{\text{fiber}}$ on the plane of the galaxy. Light from isophotes that lie within an ellipse – which is the fiber aperture projected on the plane of the disk – also contribute. The minor and major axes of this ellipse are respectively r_{fiber} and $r_{\text{fiber}}/(b/a)$. Therefore, to obtain the central luminosity within r_{circle} , the luminosity outside of this circle, but within the ellipse, would needed to be subtracted from the fiber luminosity. This “luminosity excess” increases with inclination, and is zero for face-on galaxies.

To quantify this excess, the radial distribution of in situ $\text{H}\alpha$ luminosity is needed. We adopt the findings by Hodge (1969), Hodge & Kennicutt (1983) and Athanassoula et al. (1993). These authors found in the $\text{H}\alpha$ luminosity an exponential dependence with radius, separately in two disk galaxy samples. For the half-light radius of the $\text{H}\alpha$ profile, we adopt the ratio between the half-light radius of $\text{H}\alpha$ and that of the I -band in field spirals (Koopmann et al. 2006). The ratio involving the I band is used because we can then use the half-light radius in the SDSS z band as a surrogate given their similar effective wavelengths, respectively 8062 \AA and 8931 \AA . The ratio is

$$\frac{r_{\text{eff},\text{H}\alpha}(1)}{r_{\text{eff},z}(1)} = 1.33 \pm 0.08, \quad (1)$$

and with a sample scatter of 0.52. The bracket denotes the inclination, that is face-on in this case. Similar to Paper I, we fit to apparent size vs. inclination the formula: $\log_{10} [r_{\text{eff}}(b/a)] = \log_{10} [r_{\text{eff}}(1)] - \beta \log_{10} (b/a)$. The results in Table 1 show that the apparent size increases with inclination, found previously in other studies (Huizinga & van Albada 1992; Möllenhoff et al. 2006; Maller et al. 2009, , Paper I), and shown here for the 5 SDSS bands u, g, r, i, z . The face-on half-light radius of the galaxies increases toward shorter wavelengths, consistent with the galaxies being dusty. As such, an extinction radial gradient causes an increase in the apparent half-light radius; and the extinction amplitude is larger toward shorter wavelengths. The average z band half-light radius of our galaxies, as required in Eqn. 1, is $2.89''$ (Table 1).

A numerical integration is then used to calculate the Fiber-to-Circle luminosity, $R_{\text{Fiber-to-Circle}}(b/a)$, where the surface brightness of $\text{H}\alpha$ follows an exponential profile (see Eqn. 2 below) with the half-light radius derived above. The luminosity ratio is fully determined from the axis ratio of the galaxy, the $\text{H}\alpha$ half-light radius, and the spectroscopic fiber radius r_{fiber} . We find $R_{\text{Fiber-to-Circle}}(b/a = 0.15)$ to be 2.7, decreases gradually as inclination decreases, and is unity at the face-on orientation. The value of $R_{\text{Fiber-to-Circle}}(b/a)$ is tested to depend only mildly on the $\text{H}\alpha$ -to-continuum half-light radius ratio, less than 5% change for $\approx 30\%$ change in this ratio (correspond to $1.33 \pm$ sample scatter from Koopmann et al. (2006)).

2.1.2. Step 2: Circle-to-Total Correction

We calculate in this step the Circle-to-Total $\text{H}\alpha$ luminosity by considering the total luminosity inside a radius r in a galaxy with exponential $\text{H}\alpha$ profile:

$$L(r) = \int_0^r I(r) 2\pi r dr, \quad (2)$$

$$= 2\pi I_0 \left[\frac{e^{ar}}{a} \left(r - \frac{1}{a} \right) + \frac{1}{a^2} \right], \quad (3)$$

where $I(r) = I_0 \exp(ar)$, and $a \equiv -1.68/r_{\text{eff},\text{H}\alpha}^1$. The total luminosity, $L(\infty)$, is $2\pi I_0/a^2$. The Circle-to-Total luminosity, $L(r = r_{\text{circle}} = 1.5'')/L(\infty)$, can therefore be fully determined from the $\text{H}\alpha$ half-light radius and the fiber radius only. The Circle-to-Total $\text{H}\alpha$ luminosity is determined to be 14.0%, or $R_{\text{Circle-to-Total}} = 0.14$.

Combining both corrections, the aperture-corrected line luminosity is finally

$$L_{\text{Total}}(b/a) = \frac{L_{\text{Fiber}}(b/a)}{R_{\text{Fiber-to-Circle}}(b/a) \times R_{\text{Circle-to-Total}}}. \quad (4)$$

3. Nebular Luminosity & Present Star Formation Rate as a function of Inclination

The dependence of $H\alpha$, $H\beta$, $H\gamma$, $[\text{O II}]$ and $[\text{N II}]$ luminosities on inclination are shown in Figure 1 and tabulated in Table 2. Their luminosities decrease with inclination. We deduce that this line-luminosity–inclination trend is caused by the presence of diffuse dust in the disk. The reasons are twofold. Firstly, the geometry of the dust localized to the H II regions is not expected to correlate with the disk inclination. Secondly, the relative extinction in the line luminosities is 1.2 mag, calculated from the factor of three luminosity drop in the observed inclination range. This value is consistent with the extinction in disks (Driver et al. 2007; Maller et al. 2009; Yip et al. 2010), all being derived through the inclination dependency of stellar continuum.

Fitting the luminosities with a $\log_{10}^2(b/a)$ dependence

$$\log_{10} [L(b/a)] - \log_{10} [L(1)] = -\eta \log_{10}^2(b/a) \quad (5)$$

gives η in the 0.9 – 1.1 range for these emission lines. The small range of η values is a manifestation of these lines arisen from same H II regions. The ratio of H II region emissions is, therefore, expected to remain constant with inclination (e.g., the constancy of Balmer decrement in Paper I).

We use the calibrations in Kennicutt (1998) to derive the present SFR due to O/B stars from the line luminosities. The calibrations are

$$\text{SFR} = \frac{L_{H\alpha}}{1.27 \times 10^{41} \text{ erg s}^{-1}} (M_{\odot} \text{ yr}^{-1}) \quad (6)$$

for $H\alpha$ emission, and

$$\text{SFR} = \frac{L_{[\text{O II}]}}{7.14 \times 10^{40} \text{ erg s}^{-1}} (M_{\odot} \text{ yr}^{-1}) \quad (7)$$

for $[\text{O II}]$ emission. The derived $H\alpha$ SFR are shown on the right y-axis of Figure 2. The average SFR for our disk galaxies is about $1.1 M_{\odot} \text{ yr}^{-1}$. The SFR agree well in both the $H\alpha$ and the $[\text{O II}]$ lines, as shown in Figure 3, in the inclination-to-inclination basis. This agreement is expected if the $H\alpha$ and $[\text{O II}]$ emissions arise from the same H II regions and hence the same inclination dependency. In principle, there could be H II regions embedded within the disks that cannot be observed. The nebular luminosities, and hence the present SFR, are lower limits.

Combining Eqn. 5 with Eqn. 6 and 7, the present SFR derived from $H\alpha$ follow this relation

$$\log_{10} [\text{SFR}(1)] = \log_{10} [\text{SFR}(b/a)] + 0.89 \log_{10}^2(b/a) , \quad (8)$$

and similarly for the $[\text{O II}]$ -derived SFR,

$$\log_{10} [\text{SFR}(1)] = \log_{10} [\text{SFR}(b/a)] + 0.91 \log_{10}^2(b/a) . \quad (9)$$

As in line luminosities, the SFR decreases by a factor of three from face-on to edge-on (axis ratio limit being 0.17 in our sample) galaxies. We note that, although the derivation of the SFR–inclination relations uses the correlation between line luminosity and SFR, the relations themselves do not depend on the actual values of the proportional constants in Eqn. 6 and 7.

The $[\text{O II}]/(H\alpha + [\text{N II}])$ luminosity ratio (Table 2) is found here to be about 0.4 (Table 2), in good agreement with that by Kennicutt (1992, in which the value is 0.4), and about a factor of two higher than the measurement by Hopkins et al. (2003, in which the value is 0.23).

4. Summary

We present the inclination dependency of the $H\alpha$, $H\beta$, $H\gamma$, $[\text{O II}]$, $[\text{N II}]$ nebular luminosities derived from a sample of disk galaxies in the local universe. The extinction is deduced to be caused by diffuse dust in the disks with an amplitude of 1.2 mag. The line-luminosity–inclination relation can be used to correct for extinction in SFR of inclined disk galaxies. The measuring of $[\text{O II}]$ luminosity in sky surveys – BOSS (Schlegel et al. 2007), WiggleZ (Glazebrook et al. 2007), PRIMUS (Coil et al. 2010), to name a few – would make our approach to become valuable in studying star-forming disk galaxies out to redshift of 1.6.

For the continuum-generating stars, the model-based face-on (i.e., inclination independent) extinction is in the optically thin regime (e.g., Paper I). That for the H II region emissions is not determined in this work. We are investigating this question.

5. Acknowledgments

We thank Jim Heasley, Julianne Dalcanton, Andrew Connolly, Sandra Faber, David Koo, Joel Primack, Vivienne Wild, Stéphane Charlot, Paul Hewitt, Robert Kennicutt, Aida Wofford, Carl Leitherer, Alister Graham, Tim Heckman, Brice Ménard and Rosemary Wyse for comments, discussions, suggestions.

This research has made use of data obtained from or software provided by the US National Virtual Observatory, which is sponsored by the National Science Foundation.

Funding for the SDSS and SDSS-II has been provided by the Alfred P. Sloan Foundation, the Participating Institutions, the National Science Foundation, the U.S. Department of Energy, the National Aeronautics and Space Administration, the Japanese Monbukagakusho, the Max Planck Society, and the Higher Education Funding Council for England. The SDSS Web Site is <http://www.sdss.org/>.

REFERENCES

- Adelman-McCarthy, J. K., Agüeros, M. A., Allam, S. S., et al. 2008, *ApJS*, 175, 297
- Athanassoula, E., Garcia-Gomez, C., & Bosma, A. 1993, *A&AS*, 102, 229
- Bailin, J., & Harris, W. E. 2008, *ApJ*, 681, 225
- Brinchmann, J., Charlot, S., White, S. D. M., et al. 2004, *MNRAS*, 351, 1151
- Calzetti, D., Armus, L., Bohlin, R. C., et al. 2000, *ApJ*, 533, 682
- Coil, A. L., Blanton, M. R., Burles, S. M., et al. 2010, *arXiv:1011.4307*
- Connolly, A. J., Szalay, A. S., Dickinson, M., Subbarao, M. U., & Brunner, R. J. 1997, *ApJ*, 486, L11
- Conroy, C., Schiminovich, D., & Blanton, M. R. 2010, *ApJ*, 718, 184
- Dobos, L., Budavári, T., Csabai, I., & Szalay, A. S. 2004, *Astronomical Data Analysis Software and Systems (ADASS) XIII*, 314, 185
- Driver, S. P., Popescu, C. C., Tuffs, R. J., Liske, J., Graham, A. W., Allen, P. D., & de Propris, R. 2007, *MNRAS*, 379, 1022
- Driver, S. P., Popescu, C. C., Tuffs, R. J., et al. 2008, *ApJ*, 678, L101

- Glazebrook, K., Blake, C., Couch, W., et al. 2007, arXiv:astro-ph/0701876
- Hakobyan, A. A., Petrosian, A. R., Yeghazaryan, A. A., & Boulesteix, J. 2007, *Astrophysics*, 50, 426
- Hodge, P. W. 1969, *ApJ*, 155, 417
- Hodge, P. W., & Kennicutt, R. C., Jr. 1983, *ApJ*, 267, 563
- Holwerda, B. W., Keel, W. C., & Bolton, A. 2007, *AJ*, 134, 2385
- Hopkins, A. M., Miller, C. J., Nichol, R. C., et al. 2003, *ApJ*, 599, 971
- Hopkins, A. M., & Beacom, J. F. 2006, *ApJ*, 651, 142
- Huizinga, J. E., & van Albada, T. S. 1992, *MNRAS*, 254, 677
- Kennicutt, R. C., Jr. 1992, *ApJ*, 388, 310
- Kennicutt, R. C., Jr. 1998, *ARA&A*, 36, 189
- Koopmann, R. A., Haynes, M. P., & Catinella, B. 2006, *AJ*, 131, 716
- Lilly, S. J., Le Fevre, O., Hammer, F., & Crampton, D. 1996, *ApJ*, 460, L1
- Madau, P., Pozzetti, L., & Dickinson, M. 1998, *ApJ*, 498, 106
- Maller, A. H., Berlind, A. A., Blanton, M. R., & Hogg, D. W. 2009, *ApJ*, 691, 394
- Masters, K. L., Nichol, R., Bamford, S., et al. 2010, *MNRAS*, 404, 792
- Möllenhoff, C., Popescu, C. C., & Tuffs, R. J. 2006, *A&A*, 456, 941
- Ryden, B. S. 2004, *ApJ*, 601, 214
- Schlegel, D. J., Blanton, M., Eisenstein, D., et al. 2007, *Bulletin of the American Astronomical Society*, 38, #132.29
- Shao, Z., Xiao, Q., Shen, S., Mo, H. J., Xia, X., & Deng, Z. 2007, *ApJ*, 659, 1159
- Untertorn, C. T., & Ryden, B. S. 2008, *ApJ*, 687, 976
- Wild, V., Charlot, S., Brinchmann, J., et al. 2011, *MNRAS*, 1545
- Yip, C.-W., Szalay, A. S., Wyse, R. F. G., Dobos, L., Budavári, T., & Csabai, I. 2010, *ApJ*, 709, 780 (Paper I)

York, D. G., et al. 2000, AJ, 120, 1579

Zanstra, H. 1927, ApJ, 65, 50

Table 1: Apparent size of the disk galaxies.

broadband	β^a	$\log_{10}(r_{\text{eff}}^1)^a$	r_{eff}^1 (arc-second)	$r_{\text{fiber}}/r_{\text{eff}}^1{}^b$
<i>u</i>	0.282 ± 0.010	0.550 ± 0.004	3.552 ± 0.029	0.422 ± 0.005
<i>g</i>	0.278 ± 0.008	0.508 ± 0.003	3.223 ± 0.021	0.465 ± 0.004
<i>r</i>	0.260 ± 0.007	0.485 ± 0.003	3.058 ± 0.018	0.491 ± 0.004
<i>i</i>	0.240 ± 0.007	0.476 ± 0.003	2.991 ± 0.018	0.501 ± 0.004
<i>z</i>	0.231 ± 0.007	0.461 ± 0.002	2.889 ± 0.017	0.519 ± 0.004

Note. — Galaxy apparent size increases toward shorter wavelengths.

^aThe best-fit coefficients in the adopted relation between the apparent half-light radius and the inclination. See §2.1.1.

^bThe radius of the SDSS spectroscopic fibers, r_{fiber} , is $1.5''$.

Table 2: Emission luminosity and ratio as a function of inclination.

b/a	number	[OII] λ 3728	H $\gamma\lambda$ 4341	H $\beta\lambda$ 4862	[NII] λ 6549	H $\alpha\lambda$ 6564	[NII] λ 6585	[OII]/(H α + [NII])
0.94 ± 0.03	429	7.73 ± 0.59	1.60 ± 0.28	3.81 ± 0.39	1.60 ± 0.41	14.36 ± 1.10	4.85 ± 0.58	0.37 ± 0.04
0.85 ± 0.03	759	8.31 ± 0.37	1.56 ± 0.21	3.76 ± 0.28	1.48 ± 0.34	14.22 ± 0.78	4.54 ± 0.44	0.41 ± 0.03
0.75 ± 0.03	736	7.58 ± 0.37	1.45 ± 0.20	3.49 ± 0.26	1.40 ± 0.33	13.44 ± 0.73	4.31 ± 0.43	0.40 ± 0.03
0.65 ± 0.03	729	7.78 ± 0.37	1.48 ± 0.20	3.52 ± 0.26	1.45 ± 0.32	13.80 ± 0.73	4.39 ± 0.41	0.40 ± 0.03
0.55 ± 0.03	783	6.96 ± 0.31	1.29 ± 0.16	3.10 ± 0.21	1.21 ± 0.28	12.31 ± 0.59	3.82 ± 0.34	0.40 ± 0.02
0.45 ± 0.03	806	6.59 ± 0.26	1.17 ± 0.14	2.80 ± 0.18	1.18 ± 0.26	11.51 ± 0.51	3.56 ± 0.32	0.41 ± 0.02
0.35 ± 0.03	942	4.99 ± 0.18	0.89 ± 0.11	2.13 ± 0.14	0.91 ± 0.21	9.34 ± 0.37	2.87 ± 0.24	0.38 ± 0.02
0.25 ± 0.03	828	3.53 ± 0.12	0.57 ± 0.07	1.43 ± 0.09	0.64 ± 0.15	6.67 ± 0.25	2.02 ± 0.17	0.38 ± 0.02
0.17 ± 0.02	271	2.38 ± 0.13	0.36 ± 0.06	0.91 ± 0.08	0.40 ± 0.12	4.27 ± 0.24	1.29 ± 0.14	0.40 ± 0.03

Note. — The luminosities are in units of 10^{40} erg s $^{-1}$, \pm one sigma uncertainty.

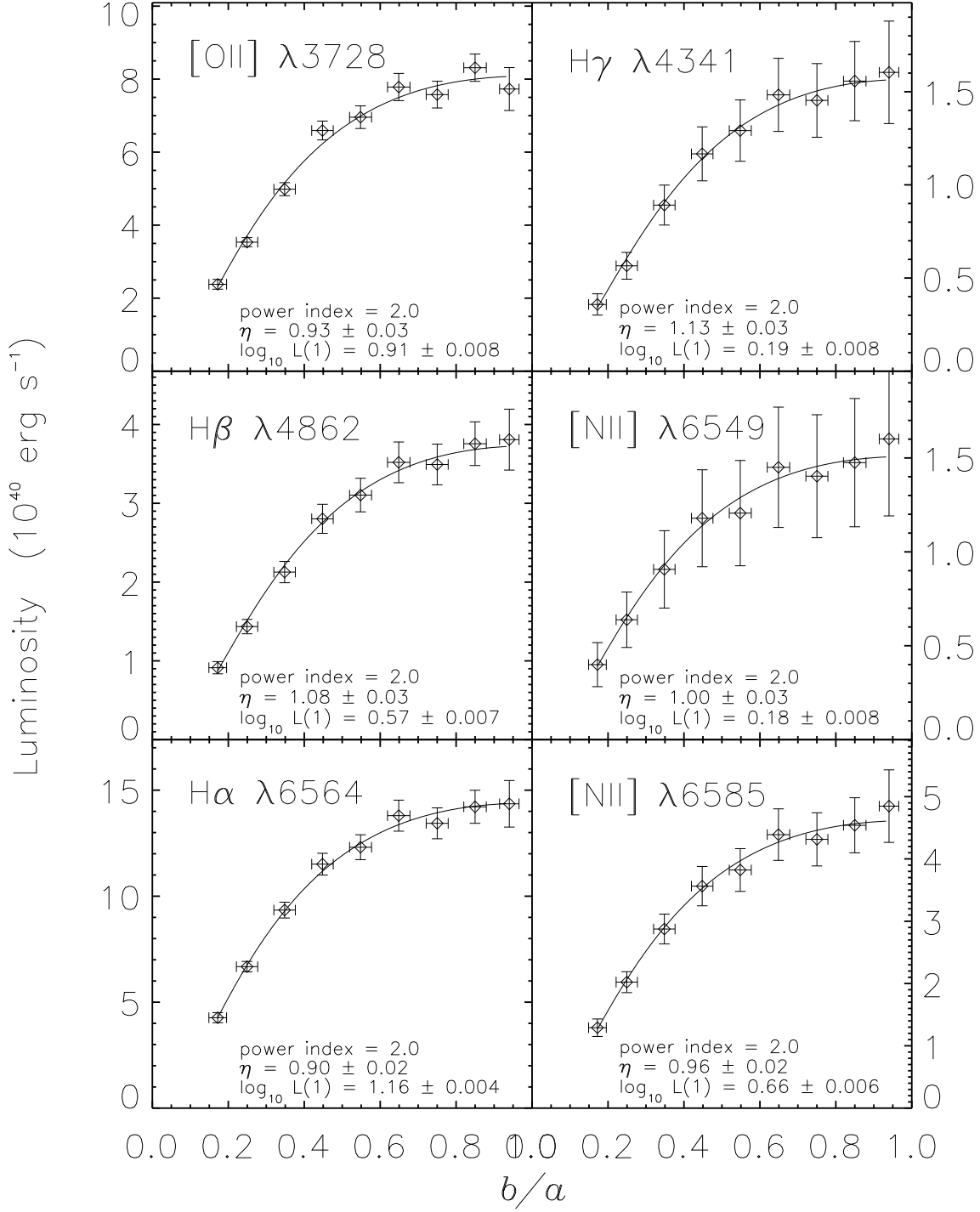


Fig. 1.— The nebular luminosities (\pm one sigma uncertainty) of the disk galaxies as a function of inclination. The solid line is the best-fit relation $\log_{10} [L(b/a)] - \log_{10} [L(1)] = -\eta \log_{10}^2(b/a)$. The legend shows the best-fit coefficients.

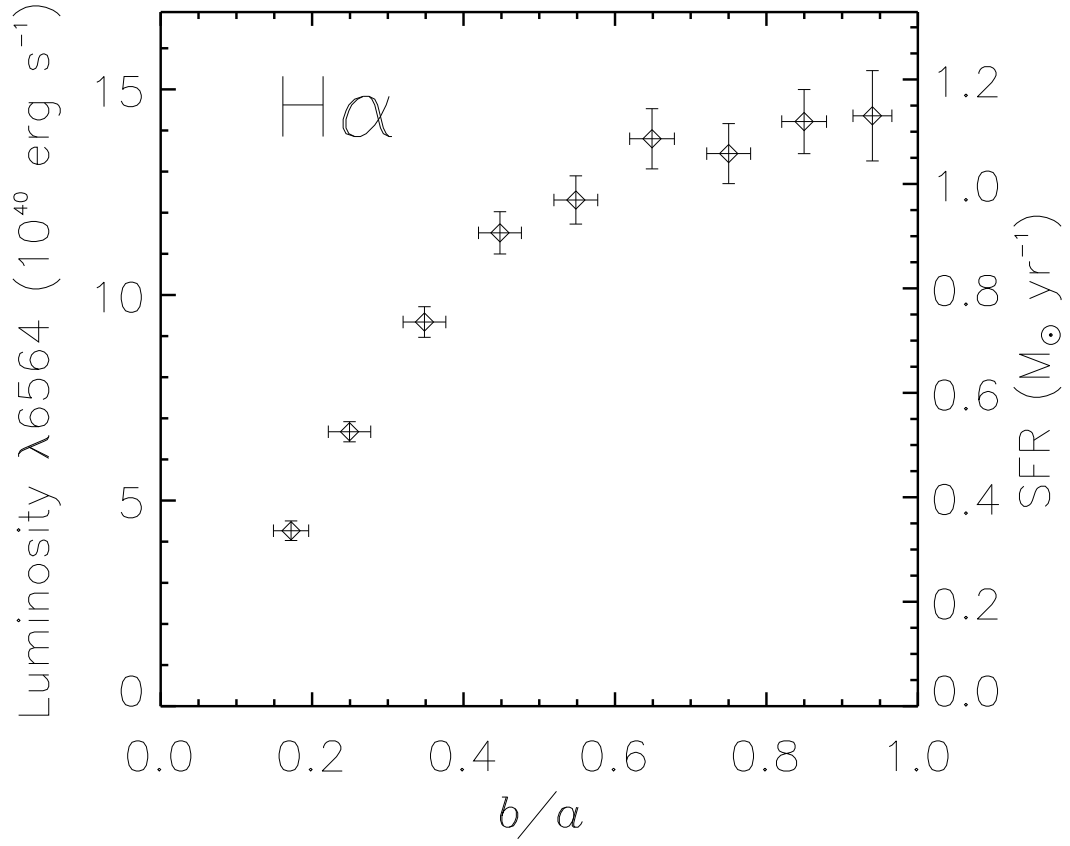


Fig. 2.— The H α luminosity (\pm one sigma uncertainty) of the disk galaxies as a function of inclination. The right y-axis shows the present SFR, converted from $L_{H\alpha}$ using Eqn. 6. The luminosity and SFR decrease by about a factor of three from face-on to edge-on orientations.

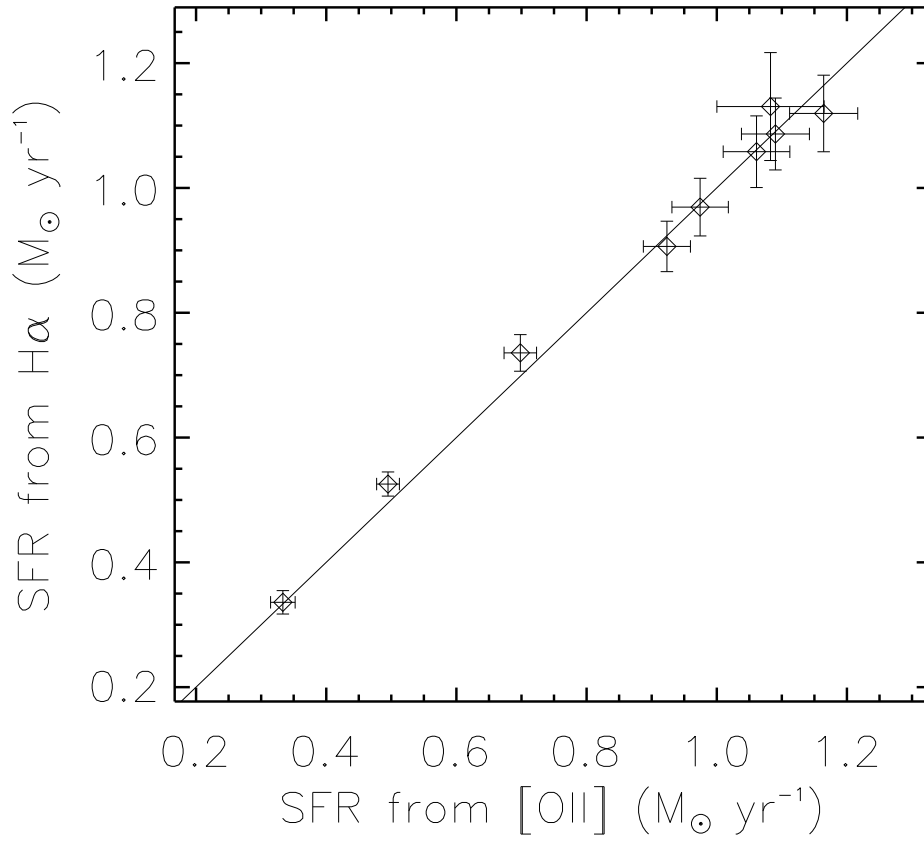


Fig. 3.— The derived SFR using [O II] and H α agree well on the inclination-to-inclination basis.